FOCAL MECHANISM OF THE 30 JUNE 1975 YELLOWSTONE EARTHQUAKE FROM TELESEISMIC SH WAVE ANALYSIS

Greg Wimpey
Department of Geology
Trinity University
San Antonio, Texas 78212

Introduction

The June 30, 1975 Yellowstone earthquake had a local magnitude M_L=6.1. This is near the lower limit of the size of earthquake that can be easily studied using teleseismic body waves. For this reason, this is one of the few events in the western United States that has not be carefully studied. The difficulty in studying this event is compounded by a poor distribution of seismic stations in the distance range between 30° and 90° that is appropriate for teleseismic body wave modeling. Although there is reasonably good coverage to the north and east, the southwest coverage is missing because these distances fall in the Pacific ocean.

Robert Andrews has studied the P waves of this event. The results of that study, as well as an overview of the tectonics of the region are presented in the previous paper in this volume. The results of that study indicated a normal faulting mechanism with a focal depth of between 2.5 and 4.0 km (Andrews, personal communication). In addition, he found that a crustal model containing a low velocity zone improved the quality of the synthetic P wave fits. The P wave analysis was unable to provide adequate constraint on the strike or slip angle of the focal mechanism. In this study, we model the SH wave seismograms of this event in an attempt to further constrain the focal mechanism.

Methods

Theoretical S wave arrival times were computed given the ISC reported epicentral location and origin time. The microfiche chips were examined and an attempt was made to locate the S arrivals. On many records the arrivals were too small to accurately identify. A set of 16 records was determined to have clear enough arrivals to digitize.

Both the north-south and east-west components of the long-period WWSSN records were digitized. The digitized records were then resampled to produce time series with identical start times and time increments. These components were then rotated (projected) to produce a radial component, along the direction of wave propagation, and a transverse component, perpendicular to the direction of wave propagation. The direction of wave propagation is computed using spherical geometry and the location of the source and receiver. The SH waves should be present only on the transverse component. The transverse components were then modeled with synthetic seismograms, and the focal mechanism parameters altered to achieve the best fit at all stations.

Results

The depth and crustal model used by Andrews (previous abstract) were used as initial starting points for the SH modeling. These parameters were observed to provide the best fits for the SH waves as well. In particular, the S waves should show as much if not more effect of the crustal low velocity zone as the P waves since both S wave velocity and attenuation are more sensitive to partial melting than the P velocity and attenuation. Synthetics were created with and without the low velocity zone. Some improvements in the fits at stations to the east were observed using the crustal model with the low velocity zone. The SH waves were best fit with a depth of 4.0 km.

The strike, dip and slip angle determined by Andrews produced acceptable fits at most stations indicating that the general mechanism was correct. However, the fits at stations to the east of the epicenter such as BEC and MAL required a change in the mechanism. The strike was rotated more nearly north, the dip was decreased slightly, and the slip angle was decreased to move these stations closer to the SH nodal lines. The best fit mechanism, based on the SH wave modeling is shown in Figure 1. The strike is N5°W, the dip is 55°E, and the slip angle is 250°. The mechanism obtained by Andrews is also plotted in Figure 1. Figure 2 shows a set of best fit synthetic and observed SH seismograms. The SH focal sphere, shown in Figure 2, exhibits SH nodal **lines** rather than P nodal **planes**. The SH nodal lines are complex geometric figures that show the directions where no horizontally polarized S waves are radiated. P wave synthetics were calculated using the revised focal mechanism parameters and were observed to be nearly iden-

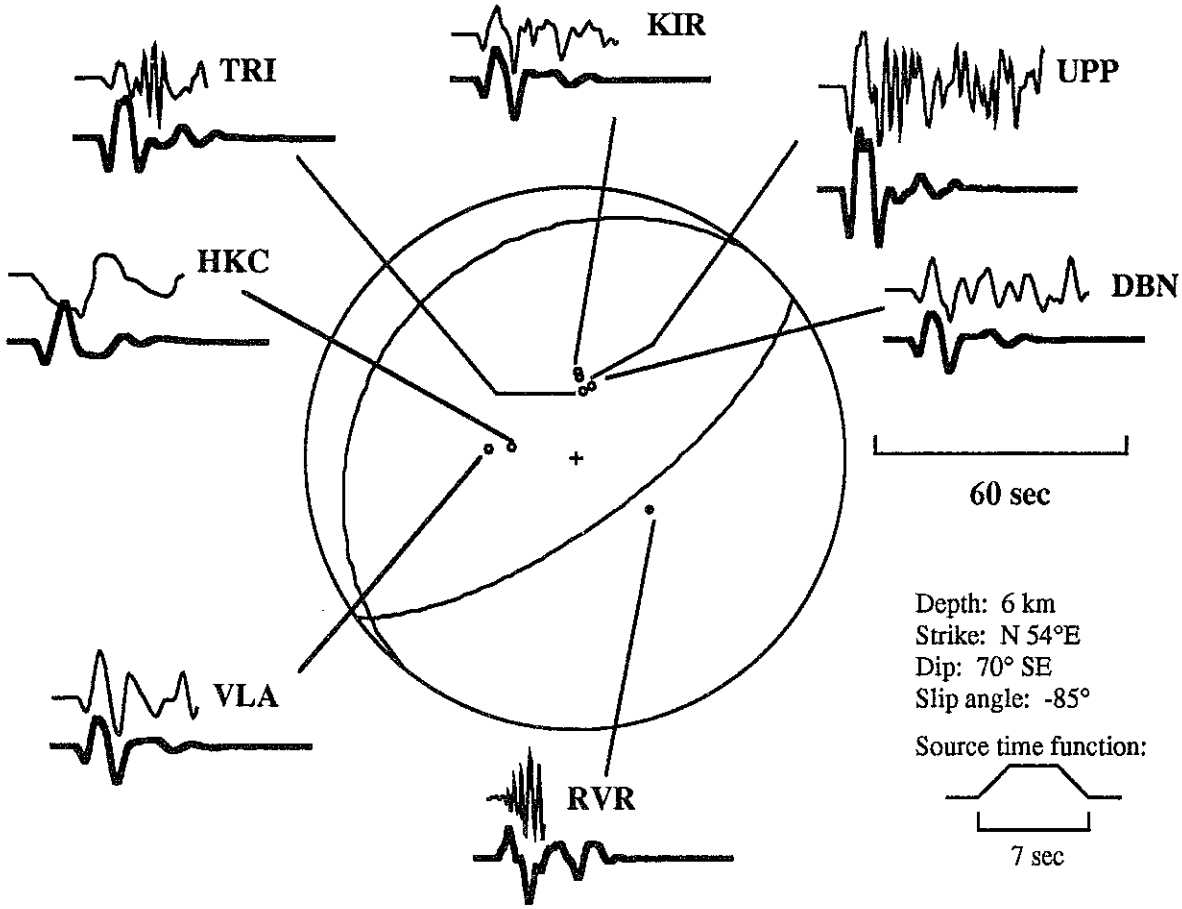

Figure 3. Observed P waves (top line) compared with synthetics (bottom line, bold). Although station HKC appears strange, the overall fit to the synthetics is good given the poor quality of the record. Because the instrument constant for station RVR is unknown, it is primarily valuable for polarity.

DBN is De Bilt, Netherlands
UPP is Uppsala, Sweden
KIR is Kiruna, Sweden
TRI is Trieste, Italy
VLA is Vladivostok, U.S.S.R.
HKC is Hong Kong
RVR is Riverside, California

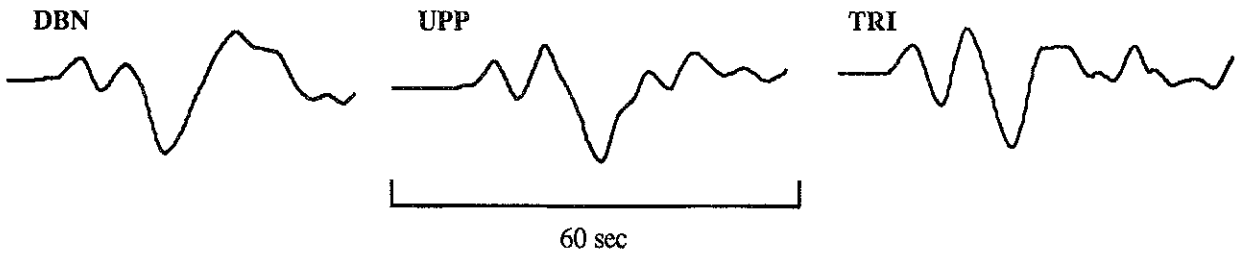

Figure 4. The SH wave forms from the European stations look strikingly similar. However, the depth which creates best fits for the P waves does not produce the second large trough observed in the above records.

tical to those obtained by Andrews.

For all SH wave synthetics, the best average source time function obtained by Andrews was used. This consisted of a symmetrical trapezoidal time function with rise time of 3 seconds and an overall duration of 7.5 seconds. Unlike the P waves, the SH waves did not show a variation of source duration with azimuth. This is due to the longer period nature of the S waves.

Discussion

Modeling of the SH waves of the 30 June 1975 Yellowstone earthquake, produces a mechanism that agrees with the P wave mechanism obtained by Andrews in depth, crustal structure and average source time function. In particular, the effects of the low velocity zone in the crust are clearly visible in the SH waveforms. A best fit SH mechanism has a fault plane striking more northerly than the P wave solution, and a smaller slip angle. Both of these parameters were poorly constrained by the P wave modeling so there is no contradiction present. The best fit SH wave solution, obtained using the P wave solution as a starting point, provides the best overall fit for both data sets and thus represents the best mechanism that can be obtained using body wave modeling. The poor station coverage and small size of the earthquake make this a difficult mechanism to constrain. Although the mechanism obtained here is reliable, more constraints, particularly on strike would be useful. To this end, attempts are now underway to measure the surface wave radiation pattern of this event in order to more accurately determine the focal mechanism.

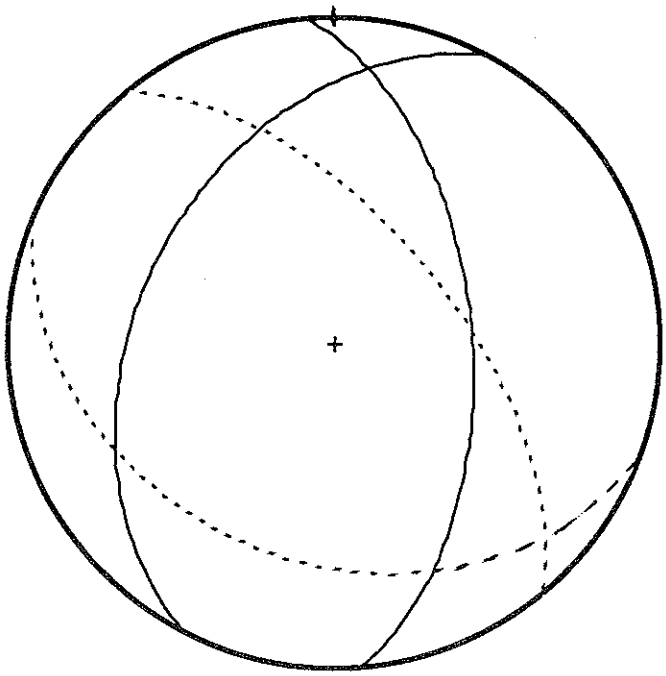

Figure 1. Best fit focal mechanism determined from SH wave synthetics. The P wave nodal planes are plotted here. The dashed planes represent the solution obtained by Andrews using only the P wave records.

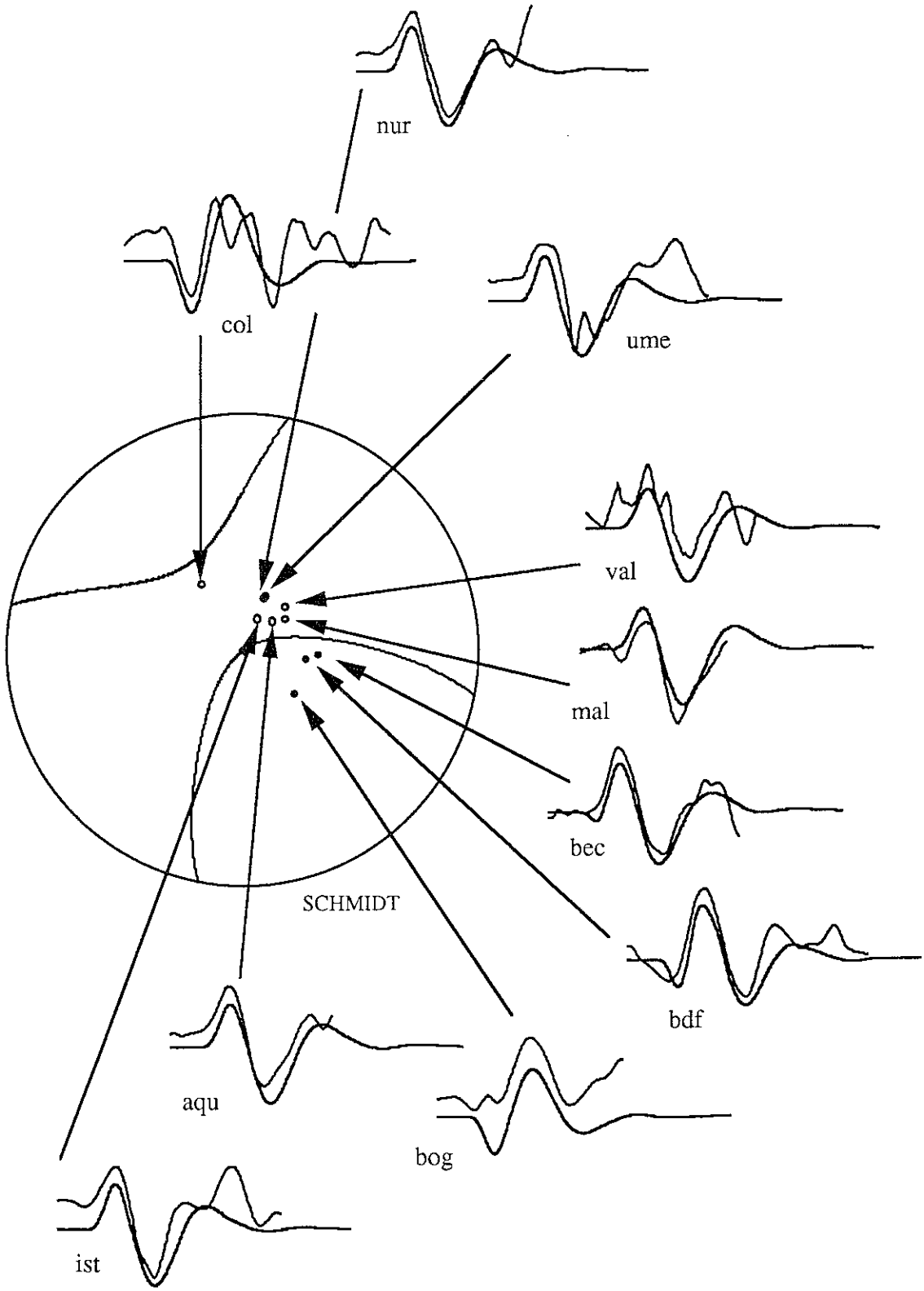

Figure 2. Best fit SH wave synthetics for the 30 June 1975 Yellowstone earthquake. At each station, the synthetic seismogram is plotted beneath the digitized observed seismogram.